Optimal resource allocation for the transport of multi-modal visual-haptic metaverse flows in 5G

Jorge Mirande, Tijani Chahed, Salah Eddine Elayoubi

▶ **To cite this version:**

Jorge Mirande, Tijani Chahed, Salah Eddine Elayoubi. Optimal resource allocation for the transport of multi-modal visual-haptic metaverse flows in 5G. Wireless Communications and Networking Conference (WCNC), Mar 2025, Milan, Italy. hal-04791648

HAL Id: hal-04791648
https://hal.science/hal-04791648v1

Submitted on 20 Nov 2024

HAL is a multi-disciplinary open access archive for the deposit and dissemination of scientific research documents, whether they are published or not. The documents may come from teaching and research institutions in France or abroad, or from public or private research centers.

L'archive ouverte pluridisciplinaire **HAL**, est destinée au dépôt et à la diffusion de documents scientifiques de niveau recherche, publiés ou non, émanant des établissements d'enseignement et de recherche français ou étrangers, des laboratoires publics ou privés.

Optimal resource allocation for the transport of multi-modal visual-haptic metaverse flows in 5G

Jorge Mirande*†, Tijani Chahed*, Salah Eddine Elayoubi†
* Télécom SudParis, Institut Polytechnique de Paris, SAMOVAR, Palaiseau, France
† CentraleSupélec, Université Paris-Saclay, CNRS, L2S, Gif-sur-Yvette, France

***Abstract*—We study resource allocation for a metaverse user in 5G networks and beyond. To ensure an immersive experience, one should consider the multi-modality nature of the metaverse, where each user generates multiple coupled flows, namely visual and haptic, characterized by joint Quality of Service (QoS) requirements, for instance in terms of subjective Just Noticeable Difference (JND) metric. These flows can be transported via various 5G services, such as Ultra Reliable Low Latency Communications (URLLC) for the haptic flow and enhanced Mobile Broadband (eMBB) for the visual one. Furthermore, the metaverse user has to share the radio resources with classical eMBB users, characterized by an elastic nature. We formulate an optimization problem that determines the optimal resource sharing between flows, under various performance constraints. We show how to solve this problem in real-world scenarios where there is a discrete set of modulation and coding schemes (MCSs) and considering the various characteristics of the different flows.**

I. Introduction

The metaverse refers to a virtual world wherein avatars engage in political, economic, social and cultural activities, acting as the physical user's alter ego [1]. It provides an immersive experience, considered as a collaborative space between service providers and users, transcending geographical limitations and facilitating interactions that are, otherwise, unfeasible in the physical world [2].

To access the metaverse, users can employ various immersive technologies in the framework of extended reality (XR) that includes all these technologies and is the medium that connects avatars in the metaverse and users in the real world [1]. For these interactions to occur, it is essential to engage the users' senses according to context and service, and ensure a Quality of Experience (QoE) in the metaverse [3].

While recognizing XR as a medium, the metaverse requires advanced network capabilities such as high bandwidth, end-to-end congestion control, guaranteed Quality of Service (QoS) and ultra-low latency [2]. The industrial metaverse, in turn, consists of multiple subsystems for sensing, communication and control to conduct effective data analysis and virtualized operations through digital platforms [4]. In this context, 5G is an essential building block, providing support for a range of use cases that need wireless connectivity [5].

Our objective in this paper is to optimize the resource allocation for the metaverse service, considering its multi-modal nature, i.e., one user can generate multiple concurrent flows, for instance visual and haptic, and the fact that it has to share the resources with classical single-link users. While the metaverse haptic flow has stringent delay and reliability requirements and should be served using the Ultra Reliable Low Latency Communications (URLLC) 5G service, the visual flow required high data rate and is carried using the enhanced Mobile Broadband (eMBB) service. The main difficulty is that the flows composing the metaverse traffic are inter-correlated, as they combine for an immersive experience.

A. Related work

The coexistence of the 5G services has already been studied in previous works [6]–[9]. In [6], the authors propose a communication-theoretic model that captures the three 5G services (URLLC, eMBB and massive Machine Type Communications (mMTC)), while comparing the orthogonal and non-orthogonal slicing, for differences in reliability, latency and number of supported devices. This, however, assumes that each service operates independently, ignoring the case of multi-modality between flows. In [7], the authors studied the rate loss associated with eMBB while transmitting URLLC packets, considering specific models for the rate loss due to puncturing URLLC traffic in eMBB mini slots. In [8], the focus was to maximize the eMBB transmission rate by performing a risk-sensitive optimization problem. In [9], the authors proposed a stochastic reliability analysis Modulation and Coding Scheme (MCS) selection for URLLC traffic while minimizing the throughput loss on the eMBB connections. In all these works, the focus was on the transmission rate of eMBB while ensuring decoding success probability for URLLC, without addressing the possible concurrency of flows for the same user.

To provide a feeling of immersion within the metaverse, the authors in [3] propose an attention-aware allocation scheme for extreme URLLC (xURLLC). [10] studies an incentive mechanism and reinforce immersion in Virtual Reality (VR). Additionally, the authors in [11] include a human-centric approach to ensure a sufficient QoE focusing on eMBB traffic. Again, these approaches in resource allocation focus on a single type of service and not on the concurrent influence for a visual-haptic immersive experience.

The multiple service concurrency was first addressed in [12], where the authors introduced the notion of a user with dual visual-haptic concurrent links, combined by the notion of Just Noticeable Difference (JND), nonetheless, omitting the presence of other types of users within the network and restricting the analysis to dense networks.

B. Focus and contributions

In this work, we focus on the resource allocation to support both the metaverse and classical single-link users. We consider a realistic scenario where each user can access a discrete set of MCSs and use the concept of JND to ensure an immersive experience. The contributions of this work are as follows:

- We provide a framework for visual-haptic metaverse user based on discrete sets of MCSs.
- We formulate and solve the optimization problem of frequency allocation while considering the needs of both the metaverse and single-link users. We ensure a sufficient immersive experience for the metaverse user and support the traffic generated by the classical single-link users.
- We study the feasibility of the problem in terms of the given spectrum as well as the MCSs availability, and provide guidelines on the optimal selection of the MCSs.

C. Paper organization

Section II details notions of visual-haptic perception and resource allocation. Section III presents the formulation of the optimization problem, discusses the feasibility and proposes the solution and algorithm of this optimization problem. Section IV shows the numerical results. Lastly, section V concludes the work and presents future work perspectives.

II. Visual-haptic system and model

The QoE of a metaverse user relies heavily on the feeling of immersion and smoothness [3]. To achieve this, the senses involved must receive the stimuli in a coordinated manner. Visual input demands a high data rate $\sim$ 10 Mbps and a packet error rate (PER) of $10^{-1} \sim 10^{-3}$. Haptic information requires a fixed data rate between $128 \sim 400$ Kbps, with high reliability, i.e., a PER of $10^{-4} \sim 10^{-5}$ [13]. Given the distinct requirements of visual and haptic stimuli, it is crucial to provide a dedicated link for each of these services. For a metaverse user, a first link, which we term link 1, is assigned to the haptic information, using URLLC [14]. Then, a second link, link 2, will be used for the visual information through eMBB [13]. Other users will also share the resources with the metaverse user, but they will only have an eMBB link individually.

Since the metaverse user will experience both visual and haptic inputs, it is necessary to introduce a metric to measure this combined visual-haptic information as a global stimulus. To ensure an immersive user experience in terms of visual and haptic stimuli, we will make use of the JND [12].

A. Just noticeable difference principle

The JND is the minimum quantity of change that results in a variation in the sensorial experience, detectable during 50% of the trials [15]. For the metaverse user, we refer to the haptic JND as γ_1 and the visual JND as γ_2. Both the visual and haptic JND follow a linear relationship with the PER [15], [16]. Additionally, for this metaverse user on each link $i \in \{1,2\}$, the PER can be defined as the complementary probability of the decoding success probability denoted by η_i. Then, we can obtain the relationship between the JND and decoding success probability as $\gamma_1 = (1-\eta_1)$ and $\gamma_2 = (1-\eta_2)$ for the haptic and visual links, respectively.

The noise variances of both the visual and haptic stimuli do not independently affect human perception; rather, they are combined in the human brain as the harmonic average of each of the stimuli [17]. Since each noise variance is proportional to their JND, for the metaverse user the joint JND for visual-haptic stimulus denoted as γ_{12} follows $\gamma_{12}^{-2} = \gamma_1^{-2} + \gamma_2^{-2}$ [17]. Therefore, the integrated visual-haptic JND for the metaverse user can be obtained from their decoding success probabilities η_i, $i \in \{1,2\}$ [12],

$$\gamma_{12}^{-2} = (1-\eta_1)^{-2} + (1-\eta_2)^{-2}. \tag{1}$$

B. Resource allocation

The Base Station (BS) allocates resources differently for users receiving visual-haptic information compared to those accessing single-link services. The total bandwidth used by the users external to the visual-haptic environment is denoted as W_E, and the one given for the metaverse users is denoted as W_M. We will consider that the BS has a total $W_T = W_M + W_E$ available bandwidth, which will be distributed among the metaverse user over the 2 links, and the single-link users. Let w_i be the amount of Physical Resource Blocks (PRB) allocated to the metaverse user on each link i:

$$W_P \sum_{i=1}^{2} w_i = W_M \tag{2}$$

where W_P is the size in Hz of a single PRB.

C. System capacity

The radio conditions depend on the user's channel conditions. Since the metaverse user on each link i can have different decoding success probability requirements η_i, they must utilize an appropriate MCS that ensures the required PER. Then, the optimal MCS will be determined based on the relationship between η_i and the Signal-to-Noise Ratio (SNR) of the metaverse user, denoted by S.

In particular, for each of the links, visual and haptic, the set $\mathcal{M}_i = \{m_1, m_2, ..., m_{M_i}\}$ will be the set of available MCS in link i and M_i the index of the last available MCS in that set. As commonly adopted in standards [18], we will consider that the available MCS are ordered from the one with the lowest spectral efficiency to the one with the highest spectral efficiency. For the metaverse user on link i the average transmission rate will be the following;

$$R_i = W_P \, w_i \, \eta_i \, f(m(\eta_i, S)) \tag{3}$$

where $f(m(\eta_i, S))$ is the spectral efficiency of the MCS which complies with the required η_i and S on link i.

We will consider that single-link users have access to the same available MCSs as the metaverse user on link_2 ($\mathcal{M}_2$). Let p_k be the proportion of single-link users whose SNR translates in using MCS $m_k \in \mathcal{M}_2$.With this, we can calculate

the capacity of the cell for the eMBB users as the harmonic average of the spectral efficiencies of each of the MCSs weighted by the fraction of users using this MCS, times the bandwidth available for the eMBB users W_E. This capacity of the cell for eMBB only users is given by [19] [20]:

$$C_E = \frac{W_E}{\sum_{k=1}^{K} p_k / f(m_k)} = W_E E_E, \tag{4}$$

where E_E is this harmonic average of the spectral efficiencies of each of the available MCSs for eMBB.

III. Optimal resource allocation

A. Optimization problem formulation

Our objective is to maximize the transmission rate of the visual information for the metaverse user, and the maximal capacity of the eMBB users connected to the BS while respecting the constraints on the limited spectrum and considering the service requirements for all users. URLLC only users are not going to be considered in the sequel, since given their fixed usage of the spectrum, they do not provide further insight into the optimization problem. For the metaverse user and the eMBB only users, we will comply with the following restrictions summarized in the optimization problem **P1**,

$$\begin{aligned}
\textbf{P1:} \max_{w_i,\eta_i} \quad & \alpha R_2 + (1-\alpha)(C_E - \lambda_E) && (5)\\
\text{s.t} \quad & R_1 = \hat{R}_1 && (6)\\
& R_2 \geq \hat{R}_2 && (7)\\
& 0 < \gamma_{12} \leq \hat{\gamma}_{12} && (8)\\
& 0 < \hat{\eta}_2 \leq \eta_2 < \eta_1 < 1 && (9)\\
& C_E > \lambda_E && (10)
\end{aligned}$$

where Eq. (5) is the objective function in terms of the average transmission rate of the visual information of the metaverse user, R_2, and the throughput of the eMBB only users, both weighted by the variable $\alpha \in [0, 1]$. In that same equation, λ_E denotes the traffic generated by the eMBB users and C_E the capacity of the cell for the eMBB connections (Eq. (4)).

Since the haptic service requires a fixed rate, the metaverse user transmission rate on link 1, say R_1, has to be equal to a target value, say $\hat{R}_1$ (Eq. (6)). For the visual information, we have to ensure at least a minimal coding rate, which translates into a minimal required throughput $\hat{R}_2$ on link 2 (Eq. (7)).

The metaverse user must reach an expected joint JND to ensure that the immersion experience in the metaverse is provided. This JND, noted as γ_{12}, has to be smaller or equal to a target visual-haptic JND denoted as $\hat{\gamma}_{12}$ (Eq. (8)). Furthermore, as the haptic PER is known to be smaller than the PER for the visual information [13], the decoding success probability on link 2, η_2, will be smaller than that of link 1, η_1. At the same time, on link 2 we will also need to ensure a minimum decoding success probability $\hat{\eta}_2$ (Eq. (9)).

Lastly, as a stability condition for the eMBB only users, we will consider that the capacity of the system for the eMBB users, C_E, is sufficient enough for the amount of traffic generated by these users, λ_E, as shown in Eq. (10).

By having the number of PRBs of the metaverse user w_i on each link i, we will also know the total share of the spectrum given to this user W_M, and in consequence the share of the spectrum that is given to the eMBB only users W_E. Then, the optimization variables of **P1** will be the decoding success probability η_i and the number of PRBs w_i.

Using the equations of the throughput Eq. (3) and the capacity of the eMBB users Eq. (4), we can reformulate the optimization problem **P1** with new optimization variables. We can rewrite the share of the spectrum used by link 2 in terms of W_M, replace the fraction of spectrum of link 1 by solving Eq. (6) and write η_1 in terms of η_2 following Eq. (1). Since the objective function is formulated for a single metaverse user, we can rewrite $R_2(\eta_2, W_M)$ following

$$R_2(\eta_2, W_M) = \left(W_M - \frac{\hat{R}_1}{\eta_1(\eta_2)\, f(m(\eta_1(\eta_2), S))} \right) \eta_2\, f(m(\eta_2, S)) \tag{11}$$

Finally, we rewrite **P1** in terms of W_M and η_2 as follows:

P2:

$$\begin{aligned}
\max_{W_M,\eta_2} \quad & \alpha R_2(\eta_2, W_M) + (1-\alpha)((W_T - W_M)E_E - \lambda_E) && (12)\\
\text{s.t} \quad & R_2(\eta_2, W_M) \geq \hat{R}_2 && (13)\\
& \left((1-\eta_1(\eta_2))^{-2} + (1-\eta_2)^{-2}\right)^{-1/2} \leq \hat{\gamma}_{12} && (14)\\
& 0 < \hat{\eta}_2 \leq \eta_2 < 1 - \sqrt{2}\,\hat{\gamma}_{12} && (15)\\
& \frac{\lambda_E}{(W_T - W_M)E_E} < 1. && (16)
\end{aligned}$$

While optimizing over W_M and η_2, we have to check the convexity of the objective function and the constraints. The objective function (12) and the constraint Eq. (13) are linear in terms of W_M, therefore convex. The inequality restriction in Eq. (16) is also a convex function in terms of W_M. On the other hand, the problem is nonconvex in terms of η_2, it is dependent on the $f()$ function which is discrete given the sets $\mathcal{M}_1$ and $\mathcal{M}_2$, and therefore nonconvex, as it happens for the restriction in Eq. (13). This non-convexity of **P2** will lead to a discrete approach based on an exhaustive search over the available MCSs for the metaverse user. Lastly, Eq. (14) and Eq. (15) are concave and convex respectively in terms of η_2.

B. Feasibility of the optimization problem

While using a coverage probability approach [12], the optimal solution is to select the minimal decoding success probability for the visual link. Nonetheless, this solution is not always feasible for the following reason. When maximizing the average transmission rate on the visual link, the optimal solution generates the minimal fraction of the spectrum required for the visual information. However, selecting the minimal value of η_2 means choosing the maximum required value of η_1, given by Eq. (1). It can be verified that w_1 is a decreasing function of η_2, and when η_2 is at its minimum,

the share of the spectrum for the haptic link takes its maximal value, which will make the problem unfeasible for $\hat{R}_1$. The unfeasibility is given when the result in between parenthesis of Eq. (11) is lower than 0, indicating that the total available resources are insufficient to satisfy the haptic link. Therefore, by choosing a higher η_2 the problem might become feasible.

Considering that there are minimal requirements on the transmission rates for each of the links of the metaverse user and including the capacity required by the single-link users, we can derive the feasibility condition for the minimal required bandwidth. Given the discretization of the available MCSs on each of the sets $\mathcal{M}_1$ and $\mathcal{M}_2$ for the visual and haptic links, and following Eq. (3) we obtain the following inequality

$$\frac{\hat{R}_2/W_T}{\eta_2\, f(m(\eta_2,S))} + \frac{\hat{R}_1/W_T}{\eta_1(\eta_2)\, f(m(\eta_1(\eta_2),S))} + \frac{\lambda_E/W_T}{E_E} < 1 \qquad (17)$$

where the choice of the MCS pair affects both terms on each of the links of the metaverse user.

On the other hand, it is also necessary to verify the feasibility region for η_1 and η_2 based on the sets $\mathcal{M}_1$ and $\mathcal{M}_2$ respectively. If no available MCS satisfies the decoding success probability required for that SNR condition, we will have $\exists i \in \{1,2\} : f(m(\eta_i,S)) = 0$. Meaning that independently of the spectrum allocation, the problem is unfeasible because of the unavailability of an MCS on either of the links that complies with the decoding success probability requirements.

C. Optimization problem decomposition

As mentioned in section III-A, the objective function **P2** is linear in W_M, then, the solution is either to give the highest amount of available resources to the metaverse user or to reduce the share of the spectrum of this metaverse user to the minimum, while complying with the feasibility conditions. This decision is determined by the parameter α. If for instance

$$\alpha\eta_2 f(m(\eta_2,S)) > (1-\alpha)E_E, \qquad (18)$$

the priority will be given to the metaverse user. In this case, the metaverse user will receive the highest available amount of resources $W_M < W_T - \lambda_E/E_E$ which is independent of the other optimization variable η_2. This fixes the right term on the objective function in Eq. (12), and reduces the objective function to the maximization of the visual information of the metaverse user. This can be summarized in the reformulation **P3** of the optimization problem **P2**,

$$\textbf{P3:}\ \underset{\eta_2}{\text{maximize}} \quad R_2$$
$$\text{s.t} \quad R_2 \geq \hat{R}_2; 0 < \hat{\eta}_2 \leq \eta_2 < 1 - \sqrt{2}\,\hat{\gamma}_{12}$$

In the other case, if the inequality (18) goes the other way round, the optimal solution will be given by W_M taking a minimum value. In this scenario, the objective function is reduced to the second term, since the metaverse user is achieving $R_2 = \hat{R}_2$ for all η_2 in the feasible region. Then, the optimization problem **P2** is reformulated into **P4**,

$$\textbf{P4:}\ \underset{\eta_2}{\text{minimize}} \quad \frac{\hat{R}_2}{\eta_2 f(m(\eta_2,S))} + \frac{\hat{R}_1}{\eta_1(\eta_2)\, f(m(\eta_1(\eta_2),S))}$$
$$\text{s.t} \quad 0 < \hat{\eta}_2 \leq \eta_2 < 1 - \sqrt{2}\,\hat{\gamma}_{12},$$

where the terms of the objective function of **P4** are the fractions of the spectrum required for each of the links.

D. Optimization problem solution and algorithm

As mentioned in section III-C, the optimization problem **P2** can be decomposed into **P3** or **P4** depending on the evaluation of Eq. (18). This, in turn, depends on the channel conditions of the metaverse user and eMBB only users, as well as the set of available MCSs for the visual link $\mathcal{M}_2$. Nonetheless, to compute the optimization problem, there must exist at least a pair of MCSs that can comply with the feasibility conditions mentioned in section III-B.

Given the SNR conditions of the user, and the available sets of MCSs for each of the links ($\mathcal{M}_1$ and $\mathcal{M}_2$), it is necessary to verify that there is at least an available subset of MCSs to which the problem is feasible. At the same time, for the given value of α, we perform a subdivision of the available MCSs for the computation of the optimization problems **P3** and **P4**. Both steps can be done as a first procedure in the feasibility check of the Algorithm 1.

Algorithm 1 Resource allocation scheme

Input: $\hat{R}_1$, $\hat{R}_2$, $\hat{\gamma}_{12}$, $\hat{\eta}_2$, S, λ_E, E_E, α
procedure FEASIBILITY CHECK
  For S and $\hat{\gamma}_{12}$, compute Eq. (17) feasible sets of MCSs.
  Identify the optimization scenario by Eq. (18).
end procedure
procedure OPTIMAL η_i^*, w_i^* COMPUTATION
  if $\alpha\eta_2 f(m(\eta_2,S)) > (1-\alpha)E_E$ **then**
    $W_M^{P3} \leftarrow W_T - W_E$
    Solve **P3** by exaustive search to get solution η_2^{P3}
  end if
  if $\alpha\eta_2 f(m(\eta_2,S)) < (1-\alpha)E_E$ **then**
    Solve **P4** by exaustive search to get solutions η_2^{P4} and W_M^{P4}
  end if
  Evaluate Eq. (12) and obtain the optimal η_2^* and W_M^*
  Return to original variable w_i^* with Eq. (2) and W_P.
end procedure
Output: η_i^*, w_i^*

In a second step, we will have to solve either one or both of the two decompositions **P3** and **P4**. The search for a solution is then given by an exhaustive search over the available MCS that comply with Eq. (18) for each case. As a result, we can have three scenarios:

*a) All feasible MCS pairs fall into **P3**:* The solution is given by exhaustive search on **P3**, resulting in the local solutions W_M^{P3} and η_2^{P3}, which are also the global solutions $W_M^* = W_M^{P3}$ and $\eta_2^* = \eta_2^{P3}$ of the optimization problem **P2**.

*b) All feasible MCS pairs fall into **P4**:* The solution is given by exhaustive search on **P4**, resulting in the local solutions W_M^{P4} and η_2^{P4}, which are also the global solutions $W_M^* = W_M^{P4}$ and $\eta_2^* = \eta_2^{P4}$ of the optimization problem **P2**.

*c) There are feasible MCS pairs both in **P3** and **P4**:* The process of the previous case scenarios is repeated. Then, there is an evaluation of the local solutions (W_M^{P3}, η_2^{P3}) and (W_M^{P4}, η_2^{P4}) in Eq. (12) to obtain the global solutions W_M^* and η_2^*.

Lastly, we return to the original optimization variables of the initial optimization problem **P1** by using Eq. (2) and W_P.

IV. Numerical Results

We first start by describing the throughput models used for the numerical analysis. For the visual link of the metaverse service and for single-link users, we consider the set of available MCSs $\mathcal{M}_2 = \{$QSPK $\{1/6, 1/3, 1/2, 3/4\}$, 16QAM $\{1/2, 2/3, 3/4, 7/8\}$, 64QAM $\{2/3, 3/4\}\}$. This data provides simulated values of both the Block Error Rate (BLER) and the SNR for each of the available MCSs for eMBB. Using Eq. (3), we compute the throughput for each of the MCSs as a function of the SNR. Then, we perform a linear interpolation among the measured values obtaining the link level curves depicted in Fig. 1. We then focus on the range $\eta_2 \geq 0.9$, representing the values above the linear interpolation for a fixed decoding success probability $\eta_2 = 0.9$, shown in Fig. 1.

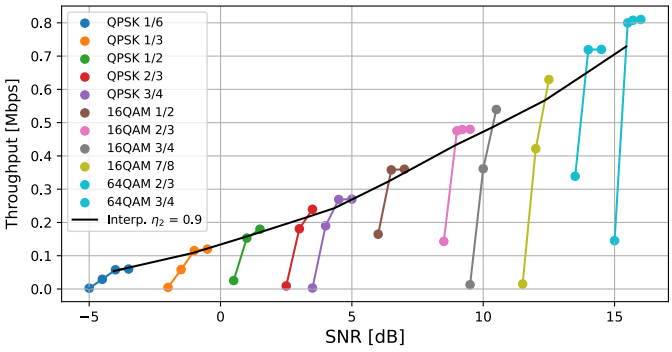

Fig. 1. Throughput of the available MCSs for the visual and eMBB links, along with its interpolation for a fixed decoding success probability $\eta_2 = 0.9$.

For the haptic link, we use the truncated exponential BLER model for an Additive White Gaussian Noise (AWGN) [9]

$$BLER_m(SNR) = \begin{cases} 1, & 0 \leq SNR < \theta_m \\ c_m e^{-d_m SNR}, & SNR > \theta_m \end{cases}$$

where c_m, d_m, θ_m are the fitting parameters obtained from table I in [9], which follows the detailed MCSs specified in 3GPP [18]. We compute the link level curves for the haptic link following Eq. (3) for the set $\mathcal{M}_1 = \{$QSPK $\{28/1024, 120/1024, 173/1024, 308/1024, 449/1024\}$, 16QAM $\{378/1024, 490/1024, 616/1024\}$, 64QAM $\{466/1024, 567/1024, 666/1024, 772/1024, 873/1024, 948/1024\}\}$. By doing this, we have both the data for the visual and haptic links in order to compute the optimization problem **P2**.

We perform the simulations with the parameters $\hat{R}_1 = 400$ Kbps, $\hat{R}_2 = 10$ Mbps, $\hat{\eta}_2 = 0.9$, $\hat{\gamma}_{12} = 2 \times 10^{-4}$ and $W_P = 180$ KHz. Considering $\alpha = 0.9$, the optimization problem **P2** follows the decomposition **P3** and is reduced to the maximization of R_2, as shown in Fig. 2. For the fixed value of $W_M = 10$ MHz, we perform the optimization problem **P3** for multiple SNR conditions. Given the finite set of available MCSs, the optimal η_2^* is given by selecting the most spectral efficient MCS, which is available for the lowest range on η_2. Additionally, Fig. 2 illustrates that for certain SNR values, the transmission rate drops to zero. This indicates that for either link 1 or 2, there is no available MCS that meets both the channel conditions and the decoding success probabilities requirements.

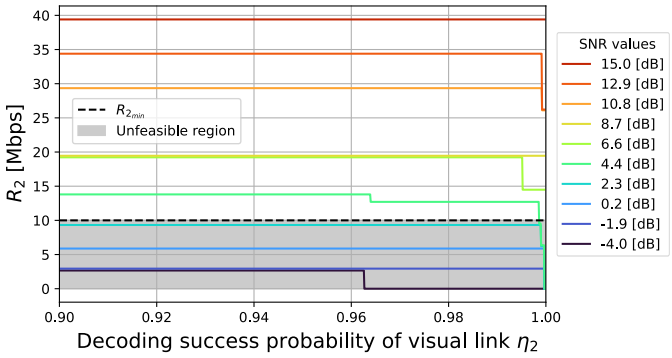

Fig. 2. Visual throughput of the metaverse user in terms of the decoding success probability of the visual link η_2. The stepped behavior is given by the discretization for a finite number of MCSs.

Next, we proceed to verify the step behavior of the non-convex restrictions for $W_T = W_M + W_E = 20$ MHz, $\lambda_E = 3$ Mbps, $p_k = 1/M_2 \ \forall \ m_k \in \mathcal{M}_2$ and $S = 4.5$ dB. While considering $\alpha = 0.2$ the optimization problem **P2**, to which the heatmap representation of the objective function is shown in Fig. 3, is reduced to **P4**. Under this scenario, the optimal solution switches to the one that gives the least available bandwidth to the metaverse user while keeping the problem feasible. For the case where $\hat{R}_1 \ll \hat{R}_2$, the selection of the MCSs is mostly given by the visual link, and the optimal point η_2^* is given by the lowest range of feasible values of η_2.

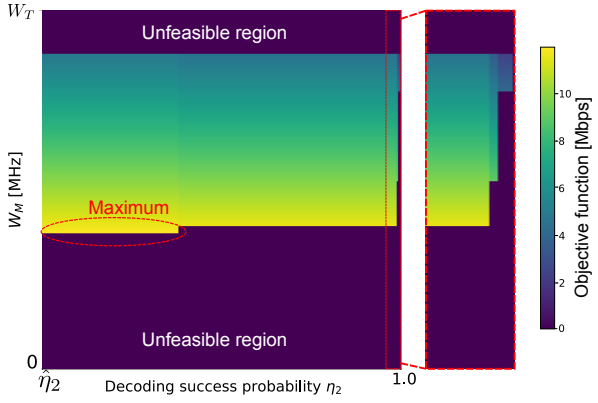

Fig. 3. Heatmap representation of the objective function for $\alpha = 0.2$. The simulation parameters are $S = 4.5$ dB, $W_T = 20$ MHz, $\hat{R}_1 = 400$ Kbps, $\hat{R}_2 = 10$ Mbps, $\hat{\gamma}_{12} = 0.0002$ and $\hat{\eta}_2 = 0.9$. The zoom in on the right side shows the fast change on the feasible MCS for higher values of η_2.

Lastly, it is relevant to mention that under these simulation

parameters, for $\alpha \sim 0.3$, there is a subset that falls into the optimization problem **P3**, while another into **P4**. Nonetheless, since the subsets falling into **P3** reach a lower W_M than those on **P4**, we know the solution will be given by η_2^{P3}, and this solution does not add further insight into the current analysis.

As mentioned in section III-D, without detailed information of the link level curves of the sets $\mathcal{M}_1$ and $\mathcal{M}_2$, an exhaustive search is necessary. Nonetheless, given the visual and haptic MCS sets, this exhaustive search can be reduced. The relative variation of the spectral efficiency between two consecutive MCSs, denoted as $\Delta f/f$, is in between $10\% \sim 30\%$ for URLLC in $\mathcal{M}_1$ and $12\% \sim 30\%$ for eMBB in $\mathcal{M}_2$. On the other hand, the relative variation of the decoding success probability denoted as $\Delta\eta/\eta$ depends specifically on the SNR conditions and the link level curves of the available MCSs.

For the haptic link, due to the high decoding success probability requirement, the relative variation $\Delta\eta_1/\eta_1$ is in the range of $\sim 10^{-4}$. Then, the choice between two MCSs is determined by the change of spectral efficiency rather than the decoding success probability given that $\frac{\Delta\eta_1}{\eta_1} \ll \frac{\Delta f}{f}$.

For the visual link, the optimal MCS can differ from the most spectral efficient one. As shown in Fig. 4, the relative optimality gap between the optimal solution attained by exhaustive search, denoted as P^*, and the solution given by selecting the most spectral efficient feasible MCS, denoted as $\tilde{P}$, defined as $\frac{|P^*-\tilde{P}|}{P^*}$, can attain $\sim 4 \times 10^{-3}$. Nonetheless, on the range of interest of visual haptic applications, i.e., $\hat{R}_2 > \hat{R}_1$, there is no appreciable optimality gap.

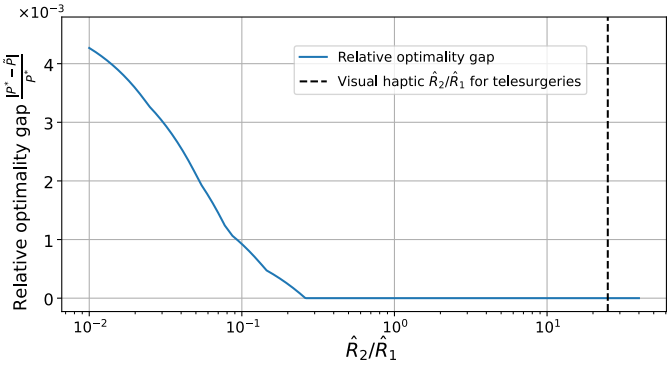

Fig. 4. Relative optimality gap for the selection of the most spectral efficient feasible MCS pair $\tilde{P}$ in comparison to the optimal solution obtained by exhaustive search, P^*. The dotted line corresponds to requirements of visual haptic ratio for telesurgery [13].

V. Conclusions

In this work, we focused on serving concurrent multi-modal metaverse services while maintaining the performance for single-link eMBB users. We modeled the interaction between visual and haptic flows using the JND approach, and formulated an optimization problem that considers the practical implementation issue of discrete sets of MCSs, where the global throughput is maximized subject to constraints on the JND, the system stability and the rates for metaverse links. We discussed the feasibility of the optimization problem and proposed a solution based on the decomposition of the problem into sub-problems. We computed and illustrated the behavior of both the objective function and feasibility regions.

In future works, we aim to study the implications of serving metaverse flows on the future network architecture, extending the concept of 5G single-service slice in the RAN [21], to a multi-modal slice serving inter-dependent flows.

References

[1] S.-M. Park and Y.-G. Kim, "A metaverse: Taxonomy, components, applications, and open challenges," *IEEE Access*, vol. 10, 2022.

[2] S. Karunarathna *et al.*, "The role of network slicing and edge computing in the metaverse realization," *IEEE Access*, vol. 11, 2023.

[3] H. Du, J. Liu, D. Niyato, J. Kang, Z. Xiong, J. Zhang, and D. I. Kim, "Attention-aware resource allocation and qoe analysis for metaverse xurllc services," *IEEE JSAC*, 2023.

[4] J. Cao, X. Zhu, S. Sun, Z. Wei, Y. Jiang, J. Wang, and V. K. Lau, "Toward industrial metaverse: Age of information, latency and reliability of short-packet transmission in 6g," *IEEE Wireless Communications*, vol. 30, no. 2, pp. 40–47, 2023.

[5] P. Hande *et al.*, "Extended reality over 5g—standards evolution," *IEEE Journal on Selected Areas in Communications*, vol. 41, no. 6, 2023.

[6] P. Popovski, K. F. Trillingsgaard, O. Simeone, and G. Durisi, "5g wireless network slicing for embb, urllc, and mmtc: A communication-theoretic view," *IEEE Access*, vol. 6, pp. 55 765–55 779, 2018.

[7] A. Anand, G. De Veciana, and S. Shakkottai, "Joint scheduling of urllc and embb traffic in 5g wireless networks," in *IEEE INFOCOM 2018 - IEEE Conference on Computer Communications*, 2018, pp. 1970–1978.

[8] M. Alsenwi, N. H. Tran, M. Bennis, A. Kumar Bairagi, and C. S. Hong, "embb-urllc resource slicing: A risk-sensitive approach," *IEEE Communications Letters*, vol. 23, no. 4, pp. 740–743, 2019.

[9] G. Saikesava and N. B. Mehta, "Mcs selection for multi-connectivity and embb-urllc coexistence in time-varying frequency-selective fading channels," in *ICC 2022*, 2022.

[10] M. Xu, D. Niyato, J. Kang, Z. Xiong, C. Miao, and D. I. Kim, "Wireless edge-empowered metaverse: A learning-based incentive mechanism for virtual reality," in *IEEE ICC*, 2022, pp. 5220–5225.

[11] J. Zhao, L. Qian, and W. Yu, "Human-centric resource allocation in the metaverse over wireless communications," *IEEE Journal on Selected Areas in Communications*, vol. 42, no. 3, pp. 514–537, 2024.

[12] J. Park and M. Bennis, "Urllc-embb slicing to support vr multimodal perceptions over wireless cellular systems," in *2018 IEEE Global Communications Conference (GLOBECOM)*, 2018, pp. 1–7.

[13] Q. Zhang, J. Liu, and G. Zhao, "Towards 5g enabled tactile robotic telesurgery," *CoRR*, vol. abs/1803.03586, 2018.

[14] P. Popovski, J. J. Nielsen, C. Stefanovic, E. d. Carvalho, E. Strom, K. F. Trillingsgaard, A.-S. Bana, D. M. Kim, R. Kotaba, J. Park, and R. B. Sorensen, "Wireless access for ultra-reliable low-latency communication: Principles and building blocks," *IEEE Network*, vol. 32, no. 2, pp. 16–23, 2018.

[15] Z. Shi, H. Zou, M. Rank, L. Chen, S. Hirche, and H. J. Müller, "Effects of packet loss and latency on the temporal discrimination of visual-haptic events," *IEEE Transactions on Haptics*, vol. 3, no. no. 1, pp. 28–36, 2010.

[16] M. Rank, Z. Shi, H. J. Müller, and S. Hirche, "Predictive communication quality control in haptic teleoperation with time delay and packet loss," *IEEE Transactions on Human-Machine Systems*, vol. 46, no. 4, 2016.

[17] M. O. Ernst and M. S. Banks, "Humans integrate visual and haptic information in a statistically optimal fashion," *Nature*, vol. 415, pp. 429–433, 2002.

[18] "Physical layer procedures for data," 3rd Generation Partnership Project, Geneva, CH, 3GPP, Jul. 2018.

[19] T. Bonald and A. Proutière, "Wireless downlink data channels: user performance and cell dimensioning," in *ACM Mobicom*, 2003.

[20] S.-E. Elayoubi, M. K. Karray, Y. Khan, and S. Jeux, "A novel hybrid simulation methodology for capacity estimation in mobile networks," *Physical Communication*, vol. 9, pp. 281–287, 2013.

[21] S. E. Elayoubi, S. B. Jemaa, Z. Altman, and A. Galindo-Serrano, "5g ran slicing for verticals: Enablers and challenges," *IEEE Communications Magazine*, vol. 57, no. 1, pp. 28–34, 2019.